Published OnlineFirst March 18, 2014; DOI: 10.1158/1940-6207.CAPR-13-0416

Research Article

Cancer Prevention Research

Classifying Patients for Breast Cancer by Detection of Autoantibodies against a Panel of Conformation-Carrying Antigens

Rick L. Evans[1], James V. Pottala[2], and Kristi A. Egland[1,2]

Abstract

Patients with breast cancer elicit an autoantibody response against cancer proteins, which reflects and amplifies the cellular changes associated with tumorigenesis. Detection of autoantibodies in plasma may provide a minimally invasive mechanism for early detection of breast cancer. To identify cancer proteins that elicit a humoral response, we generated a cDNA library enriched for breast cancer genes that encode membrane and secreted proteins, which are more likely to induce an antibody response compared with intracellular proteins. To generate conformation-carrying antigens that are efficiently recognized by patients' antibodies, a eukaryotic expression strategy was established. Plasma from 200 patients with breast cancer and 200 age-matched healthy controls were measured for autoantibody activity against 20 different antigens designed to have conformational epitopes using ELISA. A conditional logistic regression model was used to select a combination of autoantibody responses against the 20 different antigens to classify patients with breast cancer from healthy controls. The best combination included ANGPTL4, DKK1, GAL1, MUC1, GFRA1, GRN, and LRRC15; however, autoantibody responses against GFRA1, GRN, and LRRC15 were inversely correlated with breast cancer. When the autoantibody responses against the 7 antigens were added to the base model, including age, BMI, race and current smoking status, the assay had the following diagnostic capabilities: c-stat (95% CI), 0.82 (0.78–0.86); sensitivity, 73%; specificity, 76%; and positive likelihood ratio (95% CI), 3.04 (2.34–3.94). The model was calibrated across risk deciles (Hosmer–Lemeshow, $P = 0.13$) and performed well in specific subtypes of breast cancer including estrogen receptor positive, HER-2 positive, invasive, *in situ* and tumor sizes >1 cm. *Cancer Prev Res; 7(5); 545–55. ©2014 AACR.*

Introduction

For patients with breast cancer, early and personalized diagnosis is crucial for optimizing treatments leading to long-term survival. Although mammography is the most widely used method to detect breast cancer, approximately 20% of screening mammograms result in a false negative diagnosis largely because of high breast density (1). In addition, 1 in 10 women who get a mammogram will need additional imaging (2). Yet, the overwhelming majority of these women will not have breast cancer, as only 2 to 4 of every 1,000 screening mammograms leads to a cancer diagnosis (3). Therefore, there is an urgent clinical need to develop a novel, minimally invasive diagnostic strategy for the early diagnosis of breast cancer.

Measuring the levels of tumor markers, which are materials of genetic origin produced by tumors themselves or by the host in response to the tumor (4, 5), is a promising strategy for the early diagnosis of cancer. At present, there is no established tumor marker that is secreted into the peripheral circulation that can be measured by a blood test for the diagnosis of breast cancer. Currently, tumor markers that are accepted in clinical practice are tissue-based prognostic markers, such as the estrogen receptor (ER), HER-2 amplification, 21-gene Oncotype DX, and 70-gene MammaPrint (6–12). All require an invasive biopsy or surgical procedure to acquire tumor tissue for assessment, bearing a heavy burden on patients. Serum tumor markers are valuable tools that allow minimally invasive procedures for sampling to promote the early diagnosis of cancer as well as following the prognosis after treatment (4, 5). However, tumor markers produced by tumor cells usually have relatively low concentrations in the peripheral circulation, especially in early-stage disease. It has been previously shown that tumor-associated antigens (TAA) can elicit an antibody response in patients with cancer (13–15). For patients with breast cancer, several TAAs, including p53, HER-2, MUC1, HSP-60, NY-ESO-1, and c-myc, have been

Authors' Affiliations: [1]Cancer Biology Research Center, Sanford Research; and [2]Sanford School of Medicine, University of South Dakota, Sioux Falls, South Dakota

Note: Supplementary data for this article are available at Cancer Prevention Research Online (http://cancerprevres.aacrjournals.org/).

Corresponding Author: Kristi A. Egland, 2301 East 60th Street North, Sioux Falls, SD 57104. Phone: 605-312-6109; Fax: 605-312-6071; E-mail: kristi.egland@sanfordhealth.org

doi: 10.1158/1940-6207.CAPR-13-0416

Published OnlineFirst March 18, 2014; DOI: 10.1158/1940-6207.CAPR-13-0416

identified (for review, see refs. 16–18). Because the immune system can produce a considerable amount of antibody even when it is exposed to a limited amount of tumor antigen (19), the detection of antibodies against tumor proteins can be more sensitive than screening for the tumor antigens.

However, one of the largest barriers to utilizing anti-TAA antibodies as diagnostic markers is the identification of the tumor antigens recognized by the autoantibodies. Previously, serologic identification of antigens by recombinant expression cloning (SEREX) and phage display methods have been used to identify tumor antigens that elicit an autoantibody response in patients. For both methods, cDNA expression libraries were derived from cancer tissue or cell lines (20–22) and then clones encoding antigens reactive with antibodies in patients' sera were selected. Because candidate antigens are produced as denatured fragments in bacteria, the antigens lack conformational structures that represent the majority of immunogenic moieties of proteins (23–25). Membrane and secreted proteins require interactions with membrane lipids and/or posttranslational modifications, such as disulfide bond formation, for proper folding. Estimations based on available antigen–antibody complex crystal structures indicate that more than 90% of epitopes on a protein are conformational or discontinuous epitopes that form by spatial proximity (24, 25). Discontinuous epitopes consist of amino acid segments that are distantly separated in the antigen sequence and are brought into proximity by the folding of the protein. Consistent with these limitations, many of the previously identified antigens by phage display methods are nonbiologic peptides derived from noncoding sequences with questionable utility (15). Other proteomic methods for antibody detection have been developed, such as protein microarrays, reverse-capture microarrays, serological proteome analysis and nucleic acid programmable protein array (16, 26–28).

Here we report the use of a molecular approach to identify tumor antigen candidates that elicit an antibody response in patients with breast cancer. Previously, we generated a breast cancer cDNA library from membrane-associated polyribosomal (MAP) RNA, which encodes secreted and membrane proteins, and subtracted the library with RNA from normal tissues (29). Secreted proteins are more easily delivered from tumor cells to lymph nodes, where interactions of immune cells take place resulting in abundant high-affinity antibodies. Membrane surface proteins are commonly released in a soluble form from tumor cells through metalloproteinase-dependent cleavage. The shed proteins are more easily transferred to the lymph nodes than intracellular proteins (30, 31). Consequently, the obtained subtracted library, referred to as the *m*embrane-*a*ssociated *p*olyribosomal *c*DNA *l*ibrary (MAPcL), is enriched with clones encoding membrane and secreted TAA that are highly abundant in breast cancer and should preferentially induce an antibody response in patients (29). In addition, we have established a method for producing recombinant antigens as Fc fusion proteins designed to have native conformations, which is essential for the expression of membrane and secreted proteins that may induce an antibody response in patients.

We have developed a conformation-carrying antigen ELISA-based strategy to discriminate between breast cancer and healthy patients by the detection of autoantibodies against a panel of TAAs. Twenty antigens were selected from the most abundant genes represented in the MAPcL and Fc fusion proteins were generated. Blood was collected from 200 newly diagnosed patients with breast cancer and 200 healthy women as age-matched controls. The 400 plasma samples were screened for the presence of autoantibodies against the 20 different MAPcL-derived antigens using ELISA. A combination of 7 antigens with patient demographics yielded the best positive likelihood ratio to discriminate between healthy and patients with breast cancer.

Materials and Methods

Plasmid construction

For production of MAPcL-rabbit Fc-tagged antigens, 2 constructs, pSecTag2 (Invitrogen) and pFUSE-rIgG-Fc1 (InvivoGen), were both utilized to generate the 20 MAPcL-rFc expression constructs because of restriction site availability for cloning. pSecTag2 was modified by amplifying the Fc portion of rabbit immunoglobulin G (IgG) using primers 5′-CCGGATATCAGCAAGCCCACGTGCCCACC-3′ and 5′-AAGGAAAAAAGCGGCCGCTC-ATTTACCCGGAGAGCGGGAG-3′ (Integrated DNA Technologies) using pFUSE-rIgG-Fc1 as a template. The rFc PCR product was digested with *Eco*RV and *Not*I and inserted into pSecTag2, referred to as pSecTag2-rFc, which contains an IgK signal sequence for secretion. The pFUSE-rIgG-Fc1 contains an IL-2 signal sequence. To keep the signal sequence consistent between the 2 plasmids, the IgK leader sequence was amplified via PCR using pSecTag2 as a template. The IL-2 leader sequence was then replaced with the IgK signal sequence, creating pFUSE-IgK-rFc.

The accession numbers of the 20 MAPcL genes used as templates for cloning and predicted signal sequences are indicated in Table 1. The signal sequences of each encoded protein were determined using SignalP (32, 33). If a protein contained a transmembrane domain, only the encoded extracellular portion was included. The transmembrane domains were predicted using the TMHMM database (34). The amino acid numbers encoded by the cloned fragment are shown in Table 1. *ANGPTL4*, *CDH3*, *DKK1*, *SPON2*, *SSR2*, *CST2*, *GFRA1*, and *GAL1* were custom cloned into pSecTag2-rFc using the *Sfi*I and *Kpn*I restriction sites (Genscript). *EPHA2*, *IGFBP2*, and *LAMC2* were custom cloned into pSecTag2-rFc using the *Kpn*I and *Bam*HI restriction sites. *GRN*, *MUC1*, and *LRRC15* were custom cloned into pSecTag2-rFc using the *Sfi*I and *Bam*HI restriction sites. *HER-2*, *LRP10*, *SPINT2*, and *SUSD2* were cloned into pFUSE-IgK-rFc using the *Sfi*I and *Xho*I restriction sites. *CD147* was cloned into pFUSE-IgK-rFc using the *Bam*HI and *Sac*II restriction sites. *CD320* was cloned into pFUSE-IgK-rFc using the *Eco*RI and *Xho*I restriction sites.

Published OnlineFirst March 18, 2014; DOI: 10.1158/1940-6207.CAPR-13-0416

Table 1. MAPcL candidates for generation of rFc fusion proteins

Gene from MAPcL	Accession No.	Signal sequence[a] amino acids	Encoded amino acid fragment[b]
ANGPTL4	NM_139314	1–30	31–406
CD147	NM_198589	1–21	22–162
CD320	NM_016579	1–46	47–230
CDH3	NM_001793	1–24	25–654
CST2	NM_001322	1–20	21–141
DKK1	NM_012242	1–28	29–266
EPHA2	NM_004431	1–26	27–535
GAL1	NM_002305	1–17	18–135
GFRA1	AF038421	1–24	25–465
GRN	NM_002087	1–17	18–593
HER-2	NM_004448	1–22	23–652
IGFBP2	NM_000597	1–39	40–328
LAMC2	NM_005562	1–21	22–1111
LRP10	NM_014045	1–16	17–440
LRRC15	NM_001135057	1–27	28–544
MUC1	NM_002456	1–22	23–167
SPINT2	NM_021102	1–27	28–198
SPON2	NM_012445	1–26	27–331
SSR2	NM_003145	1–17	18–146
SUSD2	NM_019601	1–27	28–785

[a]The signal sequences of each encoded protein were determined using SignalP (32, 33) and were not included in the expression constructs.

[b]The amino acid numbers indicate the encoded portion of the proteins cloned between the IgG signal sequence and the Fc portion of rabbit IgG to generate the secreted MAPcL–rFc fusion proteins.

For production of His-tagged HER-2, *HER-2* was amplified via PCR using primers 5′-CCCAAGCTTGCAGCACCCAAGTGTGCACCGGCAC-3′ and 5′-GTGCTCGAGTCACGTC-AGAGGGCTGGCTCTCTGCTCG-3′. The product was digested with *Hin*dIII and *Xho*I and cloned directionally into the pET-28a expression vector.

Cell culture

293T and SKBR3 cell lines were cultured in DMEM with 10% FBS. Cultures were maintained at 37°C with 5% CO_2 in a humidified incubator. All cell lines were authenticated and tested negatively for mycoplasma.

Protein production

The MAPcL–rFc fusion proteins were produced in 293T cells. Briefly, 293T cells were transfected using Effectene (Qiagen) according to manufacturer's specifications. During transfection, the cells were cultured in DMEM with 2% FBS. Supernatants containing the secreted fusion proteins were harvested, centrifuged to clear cell debris, and supplemented with 0.1% sodium azide. His-HER-2 was produced in *Escherichia coli* (*E. coli*) BL21 (Invitrogen) and purified using IMAC affinity chromatography.

Sandwich ELISA

Microtiter plates (Nalge Nunc) were coated overnight with 2 μg/mL goat anti-rabbit Fc (Jackson Immunoresearch) diluted with phosphate buffered saline. The supernatants containing the rFc fusion proteins were diluted 1:3 serially in standard blocking buffer (0.5% bovine serum albumin and 0.1% sodium azide in PBS). Plates were washed once, and the serially diluted supernatants were transferred to the microtiter plates. Rabbit IgG of known concentration was diluted similarly and added to one row of the microtiter plate in order to quantify the amount of fusion protein present in the culture media. After incubating for 2 hours, plates were washed twice and 50 μL of horseradish peroxidase (HRP)-conjugated goat anti-rabbit IgG (Jackson Immunoresearch) diluted 1:3,000 in standard blocking buffer with 0.05% Tween 20 added. After a 2-hour incubation, plates were washed 4 times and developed with 100 μL/well of 3,3′,5,5′-tetramethylbenzidine (TMB) substrate (Pierce). The development reaction was stopped after 5 minutes with 50 μL/well of 2N H_2SO_4, and the absorbance was measured at 450 nm to determine the concentration. The absorbance at 690 nm was subtracted to remove background signal.

Antibody recognition of conformational versus denatured HER-2 protein

For the conformational HER-2 assay, microtiter plates were coated with 2 μg/mL goat anti-rabbit Fc (Jackson Immunoresearch) in PBS overnight. HER-2-ECD-rFc was then added to each well, 100 μL/well. For denatured HER-2,

Published OnlineFirst March 18, 2014; DOI: 10.1158/1940-6207.CAPR-13-0416

microtiter plates were coated with 2 μg/mL His-HER-2-ECD in PBS overnight.

Three HER-2 antibodies were used in the assay: anti-HER-2 3F27 (US Biological), anti-HER-2 3F32 (US Biological), and Herceptin (Genentech). Each antibody was diluted to 1 μg/mL in standard blocking buffer with 0.05% Tween 20. The antibodies were then serially diluted. After washing once, 50 μL/well of the serially diluted antibodies was added to the plates and incubated for 2 hours at room temperature. The plates were washed 3 times, and species appropriate HRP-conjugated secondary antibodies were added at a 1:3,000 dilution. Plates were washed 4 times and developed with 100 μL/well TMB substrate for 5 minutes. Development was stopped with 50 μL/well 2N H_2SO_4. Absorbance was measured at 450 nm, and the 690 nm absorbance was subtracted to account for background.

The same antibodies were used to stain HER-2 in SKBR3 breast cancer cells via flow cytometry. SKBR3 cells were detached from dish using Cell Dissociation Solution Non-enzymatic 1× (Sigma, catalog no. C5914). A total of 2×10^5 cells were incubated with 0.5 μg/mL of each antibody for 1 hour at room temperature. The cells were then washed, and a 1:200 dilution of PE-conjugated antibody for the appropriate species was added. The cells were again washed, resuspended in FACS buffer (PBS with 5% bovine serum albumin and 0.1% sodium azide) and analyzed by flow cytometry.

Competition of Herceptin binding

Microtiter plates were coated with 4 μg/mL goat anti-rabbit Fc and incubated overnight. After 1 wash, 100 μL/well HER-2-ECD-rFc was added to each well and incubated overnight. HER-2-Fc and CD30-Fc chimeric proteins (R&D Systems) were serially diluted from a starting concentration of 10 μg/mL. Herceptin was added to a final concentration of 10 ng/mL in each of the serial chimeric protein dilutions. Plates were washed twice, and 50 μL/well of chimeric protein/Herceptin mixture was applied to the plate. Plates were then washed 3 times, and a 1:3,000 dilution of HRP goat anti-human IgG was applied to each well, 50 μL/well. After 4 washes, 100 μL/well TMB substrate was added to each well. Development was stopped with 50 μL/well 2N H_2SO_4 after 5 minutes. Absorbance was measured at 450 nm with 690 nm absorbance subtracted.

Patients

The inclusion criteria for cases were women more than 30 years of age that were newly diagnosed with breast cancer (any type) at Sanford Health, Sioux Falls, SD. Patients were asked to provide one extra 10 mL EDTA tube of blood before mastectomy, lumpectomy, radiation therapy, chemotherapy, or other treatment. Case subjects were excluded only if they had a previous history of cancer of any kind. Healthy control subjects had a negative mammogram within 6 months before the blood draw. Healthy subjects were excluded if there was a history of previous cancer of any kind or a history of autoimmune disease. All patients provided written informed consent, and the Sanford Health IRB approved the study protocol. Blood samples from 200 patients with breast cancer were collected from October 8, 2009, to April 17, 2012. In addition, 200 age-matched healthy control blood samples were collected from October 16, 2009, to January 19, 2011. See Table 2 for enrolled patients' characteristics.

Table 2. Patient clinical and pathologic characteristics

Patients with breast cancer	***N* = 200**
Age, mean (SD)	58.9 (11.4)
White race, *n* (%)	193 (97%)
BMI, kg/m^2, mean (SD)	29.7 (6.6)
Smoking status, *n* (%)	
Current	22 (11%)
Never	120 (60%)
Past	58 (29%)
Family history yes, *n* (%)	114 (58%)
Tumor type, *n* (%)	
Invasive	148 (74%)
In situ	52 (26%)
Histology, *n* (%)	
Ductal and lobular	3 (2%)
Ductal	173 (87%)
Lobular	21 (11%)
Other	2 (1%)
ER positive, *n* (%)	171 (86%)
PR positive, *n* (%)	147 (74%)
HER-2 amplification, *n* (%)	
Negative	156 (78%)
Positive	33 (17%)
Unknown	11 (6%)
Triple negative yes, *n* (%)	18 (12%)
Tumor max dimension (cm), *n* (%)	
≤1	66 (36%)
>1 to ≤2	65 (35%)
>2	53 (29%)
Lymph node involvement, *n* (%)	47 (24%)
Age-matched controls with negative mammogram	***N* = 200**
Age, mean (SD)	58.8 (11.3)
White race, *n* (%)	192 (97%)
BMI (kg/m^2), mean (SD)	27.1 (5.5)
Smoking status, *n* (%)	
Current	7 (4%)
Never	125 (63%)
Past	67 (34%)

Serum collection

Blood was collected in a 10 mL EDTA tube and centrifuged at 2,000 × *g* for 10 minutes. Plasma was removed from the tube, aliquoted and stored at −80°C until screening for the presence of autoantibodies.

Published OnlineFirst March 18, 2014; DOI: 10.1158/1940-6207.CAPR-13-0416

Conformation-carrying antigen ELISA

Microtiter plates (Nalge Nunc) were coated overnight with 4 μg/mL goat anti-rabbit Fc (Jackson Immunoresearch) in PBS. Plates were washed once, and 100 μL/well of MAPcL–rFc fusion protein was added. Plates were incubated for 2 hours and washed twice. The plates were then coated with 50 μL/well of optimized blocking buffer (PBS with 0.5% bovine serum albumin, 0.2% dry milk, 0.1% polyvinylpyrrolidone, 20 mmol/L L-glutamine, 20 mmol/L L-Arginine, 0.1% sodium azide, 10% goat serum, and 0.05% Tween 20). The plates were incubated for 1 hour at 37°C and washed once. Serum samples diluted 1:100 in optimized blocking buffer were added and incubated for 2 hours at room temperature. Plates were then washed 3 times, and autoantibodies were detected using an HRP-conjugated goat anti-human IgG (Jackson Immunoresearch) diluted 1:3,000 in standard blocking buffer with 0.05% Tween 20. Plates were incubated for 1 hour at room temperature, washed 4 times, and developed with 100 μL/well of TMB substrate for 15 minutes. Development was stopped with 50 μL/well 2N H_2SO_4, and the absorbance was measured at 450 nm. The absorbance at 690 nm was subtracted to remove background signal. Each 96-well plate included 14 samples from breast cancer subjects and 14 samples from normal mammogram subjects. Each sample was tested in triplicate within the same plate. One row in each plate was subjected only to blocking buffer as a negative control for the ELISA (Supplementary Fig. S1).

Statistical methods

Controls were individually matched to 200 patients with breast cancer 1:1 within a 3-year age window using a greedy caliper matching algorithm (35) while blinded to assay data. For each subject, the antigen level was transformed by subtracting the mean of the blocking buffer from the mean of the triplicate measurements. If the difference was less than zero, it was set to zero, and the square root was taken to yield a more symmetrical distribution.

Differences in demographics and autoantibody responses between patients breast cancer and controls were tested using 2-sample t test and χ^2 test for continuous and categorical data, respectively. The incremental improvement to the c-statistic [i.e., concordance index, area under the receiver-operating characteristic (ROC) curve] was tested by adding the autoantibody response to each antigen to a logistic regression model that already included age, BMI, race, and current smoking status. The model calibration was tested using the Hosmer–Lemeshow goodness-of-fit measure, which constructs a χ^2 statistic by comparing the predicted and observed number of cases by probability decile (36).

After assessing the individual antigens, a multivariable conditional logistic regression analysis with strata for age-matching was used to determine the subset of antigens that minimized Akaike's Information Criterion (37); all models were adjusted for BMI, race, and current smoking status. Exploratory subgroup analyses were performed to determine if the multivariable subset of antigens performed differently in a particular type of breast cancer. The multivariable model was tested in the following subgroups: invasive, *in situ*, ER positive, tumor maximum dimension >1 cm, lymph node involvement, and HER-2 positive. The critical level α was set to $\leq 0.05/20$ antigens $= 0.0025$ using the Bonferroni correction. SAS version 9.3 software was used for all analyses.

Results

Generation of tumor-associated antigens designed to have native conformations

To identify TAAs that elicit a humoral response in patients, candidate genes that encode membrane and secreted proteins were selected from the most abundant genes represented in the MAPcL. Because only 10% of epitopes on proteins are in a linear continuous sequence (24), we utilized a eukaryotic expression system to generate conformation-carrying tumor antigens that are properly folded and contain noncontinuous epitopes for use in the detection of autoantibodies. Sequences encoding the extracellular domains (ECD) or the secreted proteins without the signal sequence of the candidate MAPcL genes were cloned 5′ of the Fc region of rabbit IgG (rFc) into the pSecTag2-rFc vector or pFUSE-IgK-rFc, depending on restriction enzyme cloning sites. The IgK leader sequence contained in the vectors directs the fusion proteins to be secreted. The vectors encoding the fusion proteins were transiently transfected into 293T cells, and the corresponding fusion proteins were secreted into the media. Production of the secreted fusion proteins was confirmed using a sandwich ELISA, and the concentrations were determined by comparison to an established CD147-rFc standard (data not shown).

To demonstrate that the generated MAPcL-rFc proteins were designed to be folded into a native conformation, an ELISA analysis was performed using commercially available anti-HER-2 antibodies generated against either native (monoclonal antibody 3F32 and Herceptin) or denatured (monoclonal antibody 3F27) HER-2 protein. Two antigens consisting of the ECD of HER-2 were analyzed: the conformation-carrying HER-2-ECD-rFc protein generated in 293T cells and a His-HER-2-ECD protein that was produced in bacteria and purified over a nickel column. The anti-native HER-2 antibody (3F32) recognized the HER-2-ECD-rFc produced in 293T (Fig. 1A), but was unable to detect the purified His-HER-2-ECD protein produced in bacteria (Fig. 1B). Also, Herceptin was unable to detect the denatured His-HER-2-ECD protein purified from bacteria (Fig. 1B). However, a strong response was observed for Herceptin when HER-2-ECD-rFc protein was used as the antigen for the ELISA analysis (Fig. 1A). Although the 3F27 antibody generated against denatured HER-2 did not detect the HER-2-ECD-rFc protein (Fig. 1A), this antibody had a strong response to bacterial HER-2-ECD (Fig. 1B).

To confirm the specific recognition of native versus denatured epitopes by the purchased antibodies, flow cytometry was performed on unfixed SKBR3 cells, a breast cancer cell line known to have HER-2 amplification (38). Because surface HER-2 would retain its native confirmation on the

Published OnlineFirst March 18, 2014; DOI: 10.1158/1940-6207.CAPR-13-0416

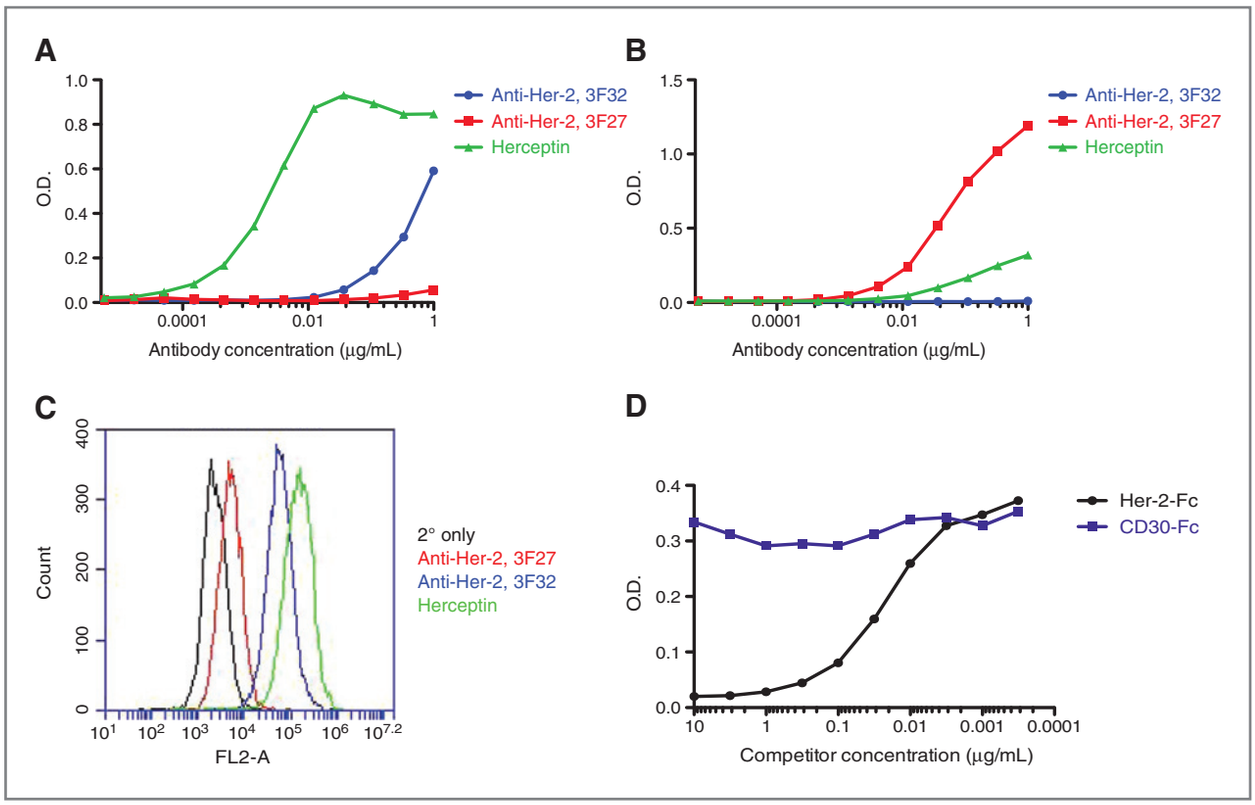

Figure 1. Antigen conformation affects antibody recognition. A, ELISA analysis using an antigen designed to have native conformation. Wells were coated with anti-rabbit IgG followed by the HER-2-ECD-rFc protein generated in 293T cells. Serial dilutions of anti-HER-2 monoclonal antibodies generated against native HER-2, 3F32 (blue), Herceptin (green), or against denatured HER-2, 3F27 (red) were used in ELISA. Reactions were developed after addition of the appropriate secondary antibody. The OD is the absorbance reading for the reaction. B, ELISA analysis using a denatured antigen. Wells were coated with purified His-HER-2-ECD generated in *E. coli*, and serial dilutions of 3F32 (blue), Herceptin (green), or 3F27 (red) were added. After addition of the secondary antibody, the reactions were developed. C, detection of native HER-2 on SKBR3 cells via flow cytometry. Fluorescence indicates antibody recognition of HER-2 on the surface of SKBR3 cells. D, binding competition assay to demonstrate specificity of conformation-carrying antigen ELISA. Wells were precoated with anti-rabbit IgG followed by HER-2-ECD-rFc. Purified HER-2-Fc (black) or CD30-Fc (purple) chimeric proteins were serially diluted and added to a constant amount of Herceptin before addition to the wells. The reactions were developed after incubation with the secondary antibody.

unfixed SKBR3 cells, the anti-HER-2 3F27 antibody, specific for denatured HER-2, was unable to detect surface HER-2 on the cell membrane of SKBR3 cells by flow cytometry (Fig. 1C). When anti-HER-2 3F32 antibody and Herceptin, both of which recognize conformational HER-2, were used for flow cytometry analysis, a large shift in fluorescence was observed indicated that the antibodies recognized HER-2 present on the membrane of the SKBR3 cells (Fig. 1C).

A binding competition assay was performed to verify that the conformation-carrying antigen ELISA was recognizing the MAPcL antigen specifically. Wells were precoated with anti-rabbit IgG followed by HER-2-ECD-rFc. Purchased HER-2-Fc and CD30-Fc purified chimeric proteins (R&D Systems) were serially diluted and added to a constant amount of Herceptin (10 ng/mL) in each well. Following the addition of the HRP-conjugated secondary anti-human IgG antibody, the reactions were developed. Herceptin binding to HER-2-ECD-rFc was competed by addition of HER-2-Fc but not the CD30-Fc protein (Fig. 1D). This result indicates that Herceptin is binding specifically to the HER-2-ECD portion of the conformation-carrying fusion protein.

Screening of patients for autoantibodies using the conformation-carrying antigen ELISA

Twenty MAPcL–rFc fusion antigens designed to contain their native conformation were generated by cloning the sequences encoding the ECD or secreted proteins 5′ of the rFc sequence (see Table 1 for identity of all 20 antigens). The expression plasmids were individually transfected into 293T cells, and the MAPcL–rFc fusion proteins were secreted into the media. The 20 fusion proteins were quantitated by sandwich ELISA analysis (data not shown). To detect autoantibodies in plasma collected from patients, a conformation-carrying antigen ELISA was developed using the generated MAPcL–rFc antigens. To immobilize the MAPcL–rFc fusion proteins, anti-rabbit IgG was used to precoat the wells of a 96-well plate. The media from the transfected 293T cells, which contains the generated MAPcL–rFc fusion proteins designed to have native conformations, was added to the precoated wells. To reduce plate variation and increase repeatability of the assay, 3 replicate samples using the plasma from each individual patient were distributed across the 96-well plate (see Supplementary Fig. S1 for

Published OnlineFirst March 18, 2014; DOI: 10.1158/1940-6207.CAPR-13-0416

Table 3. Absorbance measurements of autoantibodies and their association with breast cancer

Autoantibody	Normal mammogram ($n = 200$)	Breast cancer ($n = 200$)	*P* value[a]	OR[b]	95% CI	Increase in c-statistic[c]	*P* value
CD320	0.15 (0.12)	0.16 (0.12)	0.62	1.10	0.90–1.35	0.000	0.96
EPHA2	0.13 (0.06)	0.16 (0.10)	**0.0006**	1.64	1.21–2.24	0.034	0.037
GFRA1	0.18 (0.06)	0.20 (0.08)	0.0081	1.28	1.03–1.59	0.013	0.32
IGFBP2	0.21 (0.12)	0.25 (0.13)	**0.0006**	1.39	1.10–1.75	0.030	0.050
CST2	0.17 (0.09)	0.20 (0.10)	**0.0013**	1.39	1.12–1.73	0.026	0.13
GAL1	0.17 (0.06)	0.20 (0.07)	<**0.0001**	1.75	1.37–2.23	0.051	0.021
HER-2	0.13 (0.04)	0.15 (0.06)	<**0.0001**	1.65	1.28–2.13	0.039	0.054
LAMC2	0.15 (0.05)	0.17 (0.08)	**0.0007**	1.47	1.16–1.88	0.025	0.13
ANGPTL4	0.18 (0.05)	0.20 (0.06)	**0.0001**	1.57	1.24–1.99	0.041	0.032
DKK1	0.18 (0.10)	0.24 (0.11)	<**0.0001**	1.77	1.40–2.24	0.060	0.0093
MUC1	0.14 (0.06)	0.18 (0.08)	<**0.0001**	1.83	1.41–2.37	0.055	0.012
SSR2	0.14 (0.07)	0.17 (0.08)	**0.0007**	1.53	1.23–1.92	0.029	0.14
LRP10	0.14 (0.05)	0.15 (0.07)	0.0098	1.35	1.09–1.68	0.011	0.47
LRRC15	0.11 (0.04)	0.12 (0.05)	0.30	1.09	0.89–1.34	0.001	0.82
SPINT2	0.15 (0.07)	0.18 (0.09)	**0.0022**	1.40	1.13–1.74	0.018	0.31
SPON2	0.14 (0.07)	0.17 (0.08)	<**0.0001**	1.65	1.31–2.07	0.042	0.052
CD147	0.10 (0.05)	0.12 (0.06)	0.0039	1.43	1.15–1.78	0.016	0.38
CDH3	0.10 (0.04)	0.12 (0.04)	0.0033	1.43	1.14–1.79	0.014	0.40
GRN	0.12 (0.06)	0.13 (0.07)	0.19	1.16	0.94–1.43	0.004	0.65
SUSD2	0.12 (0.04)	0.13 (0.05)	0.0085	1.36	1.10–1.70	0.013	0.38

NOTE: Data shown as mean (SD) of $\sqrt{\text{OD} - \text{Background}}$.

[a]Differences between groups were tested using *t* tests. Significant Bonferroni adjusted *P* value < 0.05/20 = 0.0025 are shown in bold.

[b]OR (95% CI) for breast cancer prevalence per 1 SD increase in autoantibody was determined using logistic regression models adjusted for age, race, BMI, and current smoking status.

[c]Change in area under the ROC curve (i.e., c-statistic) was determined when autoantibody was added to the adjusted logistic regression models.

diagram of 96-well layout). After addition of an HRP-conjugated secondary anti-human IgG antibody, the plates were developed and the absorbance of each well was measured. The 200 plasma samples collected from newly diagnosed patients with breast cancer and plasma from 200 age-matched healthy subjects were evaluated for autoantibody reactivity against the 20 antigens using the conformation-carrying ELISA.

The 200 patients with breast cancer and 200 healthy controls had a mean (SD) age of 59 (11) years and 97% self-identified as white race (Table 2). Patients with cancer were more overweight (29.7 vs. 27.1 kg/m^2, $P < 0.0001$) and had different smoking habits ($P = 0.014$), such that there was a greater prevalence of current smokers (11% vs. 4%) in the cancer subjects versus healthy. The 200 patients with breast cancer represented the heterogeneity of the disease consisting of 74% invasive, 24% lymph node involvement, 86% ER positive, 17% HER-2 positive, and 12% triple negative breast cancer (Table 2). Analyzing the absorbance reading of the autoantibody responses against the individual antigens, we determined that there were significant Bonferroni adjusted differences between patients with breast cancer and controls in autoantibody responses against 12 TAAs, that is ANGPTL4, DKK1, EPHA2, GAL1, HER-2, IGFBP2, LAMC2, MUC1, SPON2, CST2, SPINT2, and SSR2 (Table 3). Higher levels of these autoantibodies were detected in patients with breast cancer. In logistic regression models adjusted for age, race, BMI, and current smoking status, autoantibody responses against MUC1 (1.83), DKK1 (1.77), and GAL1 (1.75; all $P < 0.0001$) had the largest OR, such that a patient was about 1.8 times as likely to have breast cancer per 1 SD increase in autoantibody response against any of these 3 antigens (Table 3). Autoantibody responses against 6 of the 12 antigens (i.e., GAL1, DKK1, MUC1, ANGPTL4, EPHA2, and IGFBP2) also increased the area under the ROC curve when each of them was added individually to the base logistic regression model adjusted for age, BMI, race, and current smoking status (all $P < 0.05$). Five of the 6 models were well calibrated across probability deciles (minimum Hosmer–Lemeshow $P = 0.13$), but the model including IGFBP2 was not calibrated ($P = 0.016$).

To increase the predictive ability of the conformation-carrying ELISA, the autoantibody response against a group of antigens was determined using conditional logistic regression analysis incorporating the individual age-matching

Published OnlineFirst March 18, 2014; DOI: 10.1158/1940-6207.CAPR-13-0416

Table 4. Multivariable logistic regression model odds ratios for breast cancer

Variable	OR (95% CI)
Age (per 1 year)	1.00[a] (0.98–1.02)
White race	0.70 (0.19–2.68)
BMI (per 1 kg/m^2)	1.09 (1.04–1.13)
Current smoking	7.88 (2.68–23.2)
ANGPTL4 (per 1 SD)	1.71 (1.16–2.50)
DKK1 (per 1 SD)	1.87 (1.28–2.73)
GAL1 (per 1 SD)	6.73 (3.42–13.3)
GFRA1 (per 1 SD)	0.41 (0.21–0.82)
GRN (per 1 SD)	0.55 (0.38–0.81)
LRRC15 (per 1 SD)	0.32 (0.19–0.55)
MUC1 (per 1 SD)	1.67 (1.16–2.41)

[a]Because of individual 1:1 age matching.

study design and adjusting for BMI, race, and current smoking status. The group with the best model fit (i.e., minimum AIC) contained the autoantibody responses against the following 7 antigens: ANGPTL4, DKK1, GAL1, MUC1, GFRA1, GRN, and LRRC15 (Table 4). Of these 7, only autoantibody responses against ANGPTL4, DKK1, MUC1, and GAL1 individually showed a significant increase in the area under the ROC curve when added to the base model (Table 3). In the fully adjusted logistic regression model including the group of antigens, current smoking had the largest OR (95% CI) of prevalent breast cancer OR = 7.88 (2.68–23.2); and BMI was also a significant risk factor OR = 1.09 (1.04–1.13) per 1 kg/m^2 increase (Table 4). GAL1 had an OR of 6.73 (3.42–13.3), so a patient was almost 7 times as likely to have breast cancer per 1 SD increase in autoantibody response against GAL1. The autoantibody responses against GFRA1 (OR = 0.41), GRN (OR = 0.55), and LRRC15 (OR = 0.32) all had inverse associations with odds of prevalent breast cancer when adjusted for responses against the other antigens (Table 4). Taken together, the autoantibody response against the group of 7 antigens increased the area under the ROC curve from 0.64 to 0.82 ($P < 0.0001$) and had the following diagnostic measures: sensitivity (72.9%), specificity (76.0%), and positive likelihood ratio (95% CI) 3.04 (2.34–3.94; Fig. 2). The model was also calibrated across risk deciles (Hosmer–Lemeshow, $P = 0.13$).

Because breast cancer is a heterogeneous disease, it is possible that the autoantibody response against a combination of antigens may categorize a subtype of breast cancer differently than analyzing all breast cancer subtypes as a whole. The breast cancer samples were grouped into individual breast cancer subtypes: invasive, *in situ*, ER positive, tumor maximum dimension >1 cm, lymph node involvement, and HER-2 positive. The ability to discriminate cases from controls in each subtype was tested using autoantibody reactivity against the 7-antigen combination in addition to age, BMI, race, and current smoking status (Fig. 2). The 7-antigen combination model performed similarly in all subtypes of breast cancer; the *c*-statistic was 0.81 to 0.85. Of the breast cancer subtypes, *in situ* tumors had the greatest area under the ROC curve (0.8520, $P < 0.0001$) when analyzed for autoantibody responses against the 7-antigen combination. The model was not calibrated when considering only those cancers with lymph node involvement because of 4 unexpected breast cancers with very low model probabilities (Hosmer–Lemeshow $P = 0.0036$).

Discussion

Early detection of breast cancer allows a physician to treat the initial stage of the disease before metastasis, thereby allowing for a higher rate of remission or long-term survival for the patient. Detecting the presence of autoantibodies generated against tumor proteins in the blood of patients would be an ideal method for breast cancer detection. However, the tumor antigens need to be identified before specific autoantibody responses in patients can be ascertained. We generated a library that encodes membrane and secreted proteins that are highly expressed in breast cancer and may elicit an immune response.

We have shown that antigen conformation alters antibody-binding affinity in our assay, and the detection of autoantibodies is limited by epitope conformation (Fig. 1). We used a robust sample set to develop the conformation-carrying ELISA consisting of 200 plasma samples collected from newly diagnosed patients with breast cancer before surgery, chemotherapy, or radiation treatment. In addition, plasma was collected from 200 age-matched subjects defined by a confirmed normal mammogram in the preceding 6 months (Table 2). All 400 plasma samples were screened individually for autoantibody response against 20 TAAs designed to contain their native conformation using ELISA. Four of the 20 TAAs analyzed in our assay have previously been reported to generate an antibody response in patients with breast cancer: MUC1 (39, 40), HER-2 (41), IGFBP2 (15), and GRN (42). Detection of autoantibodies against 12 of the 20 antigens was statistically significant for discriminating between normal and cancer samples (Table 3, bold). However, we did not observe a significant autoantibody response against GRN in our assay. Of the 12 significant antigens, 9 have not been previously associated with breast cancer autoantibodies. To our knowledge, this is the first report of the detection of autoantibodies against ANGPTL4, CST2, DKK1, EPHA2, GAL1, LAMC2, SPINT2, SPON2 and SSR2 in patients with breast cancer (Table 3).

Previously it has been shown that screening serum against a panel of antigens to detect autoantibodies compared with only a single antigen increases the sensitivity of the assay (17). This finding is consistent with the fact that breast cancer is a heterogeneous disease (43), and each individual patient's immune system is distinct. A combination of 7 TAAs, consisting of ANGPTL4, DKK1, GAL1, MUC1, GFRA1, GRN, and LRRC15, had the greatest diagnostic capability (Table 4). Compared with previously published

Published OnlineFirst March 18, 2014; DOI: 10.1158/1940-6207.CAPR-13-0416

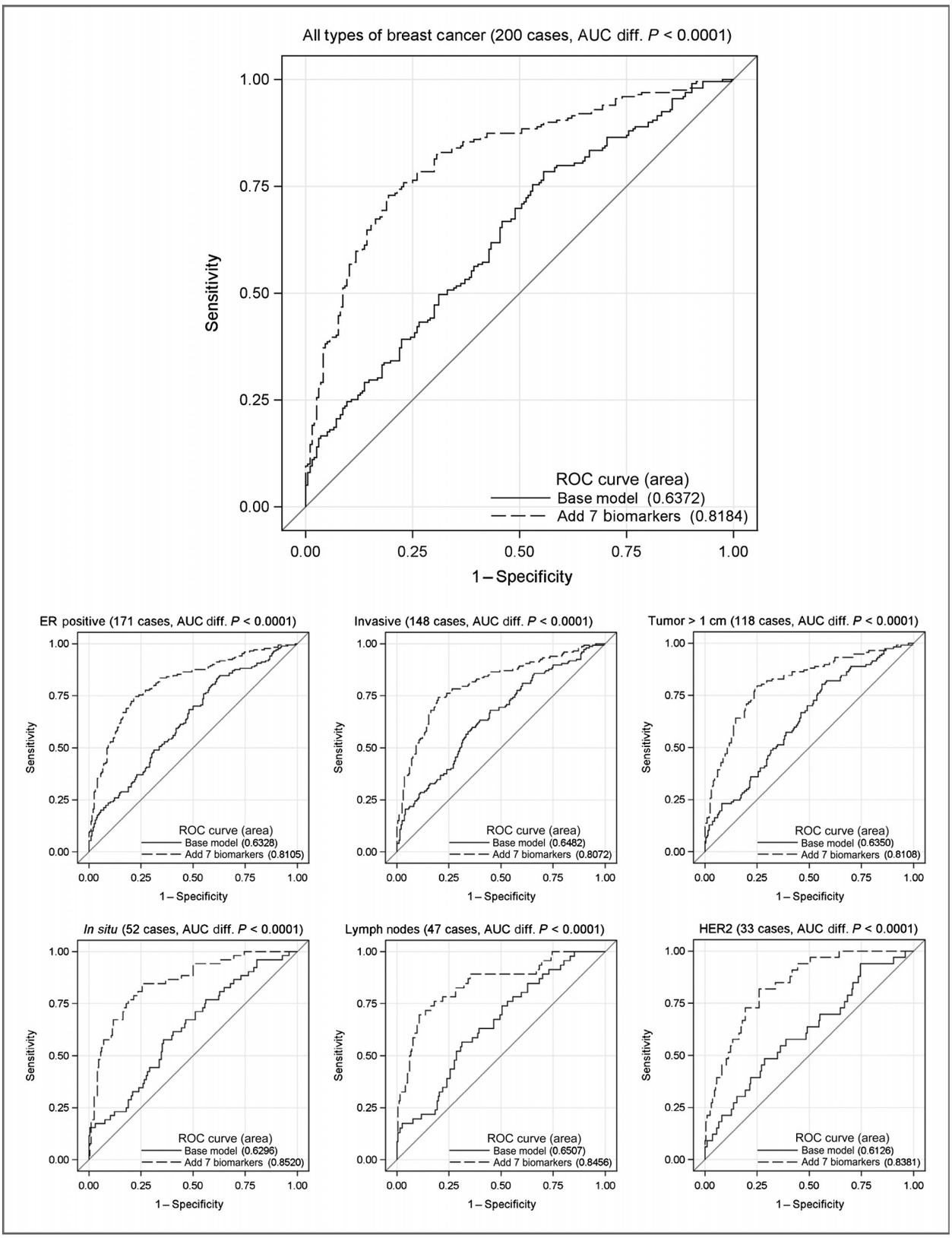

Figure 2. ROC curve comparison for classification of patients with breast cancer. The autoantibody responses against 7 antigens (i.e., ANGPTL4, DKK1, GAL1, GFRA1, GRN, LRRC15, and MUC1) were added to a logistic regression model that included age, BMI, race, and current smoking status. The ROC curves were determined for all subjects (top) and by specific subtypes of breast cancer including ER positive, invasive, maximum tumor dimension >1 cm, *in situ*, lymph node involvement, and HER-2 amplification (bottom).

Published OnlineFirst March 18, 2014; DOI: 10.1158/1940-6207.CAPR-13-0416

multiple antigen panels used to detect breast cancer autoantibodies (17, 44–46), the combination of these 7 TAAs is unique, and our study contains the largest patient population of breast cancer and healthy samples. Interestingly, in the 7-antigen combination, 4 of the antigens have statistical significance individually (Table 3), but 3 of the antigens, GFRA1, GRN, and LRRC15, were not statistically significant on their own (Table 3). However, GFRA1, GRN, and LRRC15 were inversely associated with breast cancer, indicating that lower amounts of these autoantibodies in a patient, in combination with higher levels of the directly associated autoantibodies, increased the likelihood of having breast cancer (Table 4). When the 7 antigens were added to knowledge of current smoking status and BMI, the sensitivity and specificity of the assay was 72.9% and 76.0%, respectively. The area under the ROC curve (95% CI) was 0.82 (0.77–0.85), and the positive likelihood ratio was 3.04 for the conformation-carrying ELISA. Because breast cancer is a heterogeneous disease, patients were grouped into tumor characteristics, including ER positive, HER-2 positive, *in situ*, invasive, tumor size, and lymph node involvement. The 7-antigen combination performed well for all groups (Fig. 2). These results suggest that the assay has potential clinical application. One serum recurrence marker for breast cancer that is currently used in the clinic is mucin-associated antigen CA27.29. The CA27.29 antigen is detected in the blood of a patient using a monoclonal antibody that recognizes MUC1. Because of the low sensitivity of the CA27.29 tumor marker, the test is used to follow a patient for breast cancer recurrence (47). Compared with the traditional CA27.29 tumor marker, the conformation-carrying ELISA described here shows great promise.

Currently, mammography is the standard method for breast cancer screening. However, the machinery necessary to perform a mammogram is expensive, requires specialized medical personnel to operate, and is challenging to transport to medically underserved areas. The development of a blood test for the early detection of breast cancer would greatly advance access to screening. Drawing blood is a common procedure, and blood can easily be mailed to a clinical laboratory for analysis. This study demonstrates that a combination of autoantibody responses against antigens designed to contain conformational epitopes is a promising strategy for breast cancer detection. Future studies will focus on the identification of additional antigens to improve the sensitivity and specificity of the assay for translation into the clinic.

Disclosure of Potential Conflicts of Interest

J.V. Pottala is a principal biostatistician at Health Diagnostic Laboratory Inc. No potential conflicts of interest were disclosed by the other authors.

Authors' Contributions

Conception and design: R.L. Evans, J.V. Pottala, K.A. Egland
Development of methodology: R.L. Evans, J.V. Pottala, K.A. Egland
Acquisition of data (provided animals, acquired and managed patients, provided facilities, etc.): R.L. Evans, K.A. Egland
Analysis and interpretation of data (e.g., statistical analysis, biostatistics, computational analysis): J.V. Pottala, K.A. Egland
Writing, review, and/or revision of the manuscript: R.L. Evans, J.V. Pottala, K.A. Egland
Administrative, technical, or material support (i.e., reporting or organizing data, constructing databases): R.L. Evans, K.A. Egland
Study supervision: K.A. Egland

Acknowledgments

The authors thank Dr. S. Nagata for his ideas and helpful suggestions and J. Healy, RN, for her dedication to this project and helping them consent patients into this study and obtaining blood from healthy control subjects. Sanford Clinic, Surgical Associates, was critical in the recruitment of patients. D. Smithback, RN, and G. Top, RN, are breast oncology care coordinators, and they were essential for patient recruitment. The authors also thank J. Hanisch, of the Sanford Breast Health Institute, for help in the recruitment of healthy females for control subjects, S. Jepperson and K. Fillaus for consenting patients and collecting blood in the early hours of the morning, LCM Pathology (Sioux Falls, SD) for assistance with tissue collection, Jeffrey Sachs for his stellar laboratory skills and assistance with ELISA analysis, and Dr. T. Ise for her assistance with cloning of the rFc expression constructs.

Grant Support

This research was supported by a grant from S.G. Komen for the Cure awarded to K. Egland. The Molecular Pathology, Flow Cytometry, and Imaging Cores are supported by an NIH, NIGMS, Center of Biomedical Research Excellence (COBRE) grant (1P20RR024219-01A2, to K. Miskimins).

The costs of publication of this article were defrayed in part by the payment of page charges. This article must therefore be hereby marked *advertisement* in accordance with 18 U.S.C. Section 1734 solely to indicate this fact.

Received December 2, 2013; revised February 24, 2014; accepted March 5, 2014; published OnlineFirst March 18, 2014.

References

1. National Cancer Institute at the National Institutes of Health 2012 [updated 07/24/2012; cited 2013]. Available from: http://www.cancer.gov/cancertopics/factsheet/detection/mammograms.
2. Breastcancer.org, mammography: benefits, risks, what you need to know 2013. Available from: http://www.breastcancer.org/symptoms/testing/types/mammograms/benefits_risks.jsp.
3. American Cancer Society, Find Support & Treatment, Mammograms and Other Breast Imaging Procedures 2012. Available from: http://www.cancer.org/Treatment/UnderstandingYourDiagnosis/ExamsandTestDescriptions/MammogramsandOtherBreastImagingProcedures/mammograms-and-other-breast-imaging-procedures-having-a-mammogram.
4. Agnantis NJ, Goussia AC, Stefanou D. Tumor markers: an update approach for their prognostic significance. Part I. In Vivo 2003;17:609–18.
5. Arciero C, Somiari SB, Shriver CD, Brzeski H, Jordan R, Hu H, et al. Functional relationship and gene ontology classification of breast cancer biomarkers. Int J Biol Markers 2003;18:241–72.
6. Bernoux A, de Cremoux P, Laine-Bidron C, Martin EC, Asselain B, Magdelenat H. Estrogen receptor negative and progesterone receptor positive primary breast cancer: pathological characteristics and clinical outcome. Institut Curie Breast Cancer Study Group. Breast Cancer Res Treat 1998;49:219–25.
7. Dowsett M, Cooke T, Ellis I, Gullick WJ, Gusterson B, Mallon E, et al. Assessment of HER2 status in breast cancer: why, when and how? Eur J Cancer 2000;36:170–6.
8. Shak S. Overview of the trastuzumab (Herceptin) anti-HER2 monoclonal antibody clinical program in HER2-overexpressing metastatic breast cancer. Herceptin Multinational Investigator Study Group. Semin Oncol 1999;26(4 Suppl 12):71–7.

Published OnlineFirst March 18, 2014; DOI: 10.1158/1940-6207.CAPR-13-0416

9. Slamon DJ, Clark GM, Wong SG, Levin WJ, Ullrich A, McGuire WL. Human breast cancer: correlation of relapse and survival with amplification of the HER-2/neu oncogene. Science 1987;235:177–82.
10. Slamon DJ, Godolphin W, Jones LA, Holt JA, Wong SG, Keith DE, et al. Studies of the HER-2/neu proto-oncogene in human breast and ovarian cancer. Science 1989;244:707–12.
11. Kaklamani V. A genetic signature can predict prognosis and response to therapy in breast cancer: Oncotype DX. Expert Rev Mol Diagn 2006;6:803–9.
12. Manjili MH, Najarian K, Wang XY. Signatures of tumor-immune interactions as biomarkers for breast cancer prognosis. Future Oncol 2012;8:703–11.
13. Reuschenbach M, von Knebel Doeberitz M, Wentzensen N. A systematic review of humoral immune responses against tumor antigens. Cancer Immunol Immunother 2009;58:1535–44.
14. Casiano CA, Mediavilla-Varela M, Tan EM. Tumor-associated antigen arrays for the serological diagnosis of cancer. Mol Cell Proteomics 2006;5:1745–59.
15. Lu H, Goodell V, Disis ML. Humoral immunity directed against tumor-associated antigens as potential biomarkers for the early diagnosis of cancer. J Proteome Res 2008;7:1388–94.
16. Desmetz C, Mange A, Maudelonde T, Solassol J. Autoantibody signatures: progress and perspectives for early cancer detection. J Cell Mol Med 2011;15:2013–24.
17. Piura E, Piura B. Autoantibodies to tailor-made panels of tumor-associated antigens in breast carcinoma. J Oncol 2011;2011:982425.
18. Piura E, Piura B. Autoantibodies to tumor-associated antigens in breast carcinoma. J Oncol 2010;2010:264926.
19. Finn OJ. Immune response as a biomarker for cancer detection and a lot more. N Engl J Med 2005;353:1288–90.
20. Pavoni E, Pucci A, Vaccaro P, Monteriu G, Ceratti Ade P, Lugini A, et al. A study of the humoral immune response of breast cancer patients to a panel of human tumor antigens identified by phage display. Cancer Detect Prev 2006;30:248–56.
21. Sioud M, Hansen MH. Profiling the immune response in patients with breast cancer by phage-displayed cDNA libraries. Eur J Immunol 2001;31:716–25.
22. Storr SJ, Chakrabarti J, Barnes A, Murray A, Chapman CJ, Robertson JF. Use of autoantibodies in breast cancer screening and diagnosis. Expert Rev Anticancer Ther 2006;6:1215–23.
23. Tan EM, Shi FD. Relative paradigms between autoantibodies in lupus and autoantibodies in cancer. Clin Exp Immunol 2003;134:169–77.
24. Barlow DJ, Edwards MS, Thornton JM. Continuous and discontinuous protein antigenic determinants. Nature 1986;322:747–8.
25. Laver WG, Air GM, Webster RG, Smith-Gill SJ. Epitopes on protein antigens: misconceptions and realities. Cell 1990;61:553–6.
26. Ramachandran N, Hainsworth E, Bhullar B, Eisenstein S, Rosen B, Lau AY, et al. Self-assembling protein microarrays. Science 2004;305:86–90.
27. Ehrlich JR, Qin S, Liu BC. The 'reverse capture' autoantibody microarray: a native antigen-based platform for autoantibody profiling. Nat Protoc 2006;1:452–60.
28. Tan HT, Low J, Lim SG, Chung MC. Serum autoantibodies as biomarkers for early cancer detection. FEBS J 2009;276:6880–904.
29. Egland KA, Vincent JJ, Strausberg R, Lee B, Pastan I. Discovery of the breast cancer gene BASE using a molecular approach to enrich for genes encoding membrane and secreted proteins. Proc Natl Acad Sci U S A 2003;100:1099–104.
30. Boyle JS, Koniaras C, Lew AM. Influence of cellular location of expressed antigen on the efficacy of DNA vaccination: cytotoxic T lymphocyte and antibody responses are suboptimal when antigen is cytoplasmic after intramuscular DNA immunization. Int Immunol 1997;9:1897–906.
31. Drew DR, Lightowlers M, Strugnell RA. Humoral immune responses to DNA vaccines expressing secreted, membrane bound and non-secreted forms of the Tania ovis 45W antigen. Vaccine 2000;18:2522–32.
32. Bendtsen JD, Nielsen H, von Heijne G, Brunak S. Improved prediction of signal peptides: SignalP 3.0. J Mol Biol 2004;340:783–95.
33. Nielsen H, Engelbrecht J, Brunak S, von Heijne G. Identification of prokaryotic and eukaryotic signal peptides and prediction of their cleavage sites. Protein Eng 1997;10:1–6.
34. Krogh A, Larsson B, von Heijne G, Sonnhammer EL. Predicting transmembrane protein topology with a hidden Markov model: application to complete genomes. J Mol Biol 2001;305:567–80.
35. Bergstralh EJ, Kosanke JL. Computerized matching of cases to controls. Rochester, MN: Mayo Clinic Department of Health Science Research, 1995.
36. Hosmer DW, Lemeshow S. Goodness of fit tests for the multiple logistic regression model. Communications in Statistics - Theory and Methods: Taylor & Francis Group; 1980. p. 1043–69.
37. Akaike H. Information theory and an extension of the maximum likelihood principle. In:Kotz S, Johnson NL, editors. Breakthroughs in Statistics. Springer Series in Statistics: Springer New York; 1992. p. 610–24.
38. Neve RM, Chin K, Fridlyand J, Yeh J, Baehner FL, Fevr T, et al. A collection of breast cancer cell lines for the study of functionally distinct cancer subtypes. Cancer Cell 2006;10:515–27.
39. Kotera Y, Fontenot JD, Pecher G, Metzgar RS, Finn OJ. Humoral immunity against a tandem repeat epitope of human mucin MUC-1 in sera from breast, pancreatic, and colon cancer patients. Cancer Res 1994;54:2856–60.
40. von Mensdorff-Pouilly S, Gourevitch MM, Kenemans P, Verstraeten AA, Litvinov SV, van Kamp GJ, et al. Humoral immune response to polymorphic epithelial mucin (MUC-1) in patients with benign and malignant breast tumours. Eur J Cancer 1996;32A:1325–31.
41. Disis ML, Pupa SM, Gralow JR, Dittadi R, Menard S, Cheever MA. High-titer HER-2/neu protein-specific antibody can be detected in patients with early-stage breast cancer. J Clin Oncol 1997;15:3363–7.
42. Ladd JJ, Chao T, Johnson MM, Qiu J, Chin A, Israel R, et al. Autoantibody signatures involving glycolysis and splicesome proteins precede a diagnosis of breast cancer among postmenopausal women. Cancer Res 2013;73:1502–13.
43. Perou CM, Sorlie T, Eisen MB, van de Rijn M, Jeffrey SS, Rees CA, et al. Molecular portraits of human breast tumours. Nature 2000;406:747–52.
44. Lacombe J, Mange A, Jarlier M, Bascoul-Mollevi C, Rouanet P, Lamy PJ, et al. Identification and validation of new autoantibodies for the diagnosis of DCIS and node negative early-stage breast cancers. Int J Cancer 2013;132:1105–13.
45. Mange A, Lacombe J, Bascoul-Mollevi C, Jarlier M, Lamy PJ, Rouanet P, et al. Serum autoantibody signature of ductal carcinoma *in situ* progression to invasive breast cancer. Clin Cancer Res 2012;18:1992–2000.
46. Ye H, Sun C, Ren P, Dai L, Peng B, Wang K, et al. Mini-array of multiple tumor-associated antigens (TAAs) in the immunodiagnosis of breast cancer. Oncol Lett 2013;5:663–8.
47. Gion M, Mione R, Leon AE, Dittadi R. Comparison of the diagnostic accuracy of CA27.29 and CA15.3 in primary breast cancer. Clin Chem 1999;45:630–7.

AACR American Association for Cancer Research

Cancer Prevention Research

Classifying Patients for Breast Cancer by Detection of Autoantibodies against a Panel of Conformation-Carrying Antigens

Rick L. Evans, James V. Pottala and Kristi A. Egland

Cancer Prev Res 2014;7:545-555. Published OnlineFirst March 18, 2014.